Acta Mechanica Slovaca 14 (4): 16-27, 2010
DOI: 10.2478/v10147-011-0030-z

Analysis of Thermo-Piezoelectricity Problems by Meshless Method

Jan Sládek (SK) jan.sladek@savba.sk

Vladimír Sládek (SK) vladimir.sladek@savba.sk

Peter Staňák (SK) peter.stanak@savba.sk

BIOGRAPHICAL NOTES

prof. Ing. Jan Sládek, DrSc. (born in 1952) received the degree PhD and DrSc degrees in Applied mechanics from the Slovak Academy of Sciences, in 1981 and 1990, respectively. From 1976 he is research fellow at the Institute of Construction and architecture, Slovak Academy of Sciences where he is interested in the computational mechanics with applications to mechanics of solids and fracture mechanics including multi-field problems (such as mechanical, thermal, electro-magnetic, acoustic fields). His main contribution belongs to the development of the Boundary element method (BEM), Regularization techniques in BEM, and Mesh-free methods. His teaching activities in recent two decades are oriented on applied mathematics and computational mechanics at the Slovak Technical University in Bratislava, Slovakia. His research results have been recognized several times by awarding the Slovak Academy Prize, Prize of Slovak Literary Agency. He is assoc. editor for CMES-Computer Modeling in Engineering & Sciences, member of editorial board for Jour. Computational and Applied Mechanics, member of Editorial Board of SDHM-Structural Durability and Health Monitoring Journal, member of Editorial Board of Journal of Multiscale Modelling (JMM), member of editorial board for Electronic Jour. Boundary Elements and Journal of Mechanical Engineering.

prof. RNDr. Vladimir Sládek, DrSc. (born in 1954) received the degree RNDr. (Dr. Rer. Nat.) in Pyhsics from the Comenius University in 1978, PhD and DrSc degrees in Applied mechanics from the Slovak Academy of Sciences, in 1984 and 1990, respectively. From 1981 he is research fellow at the Institute of Construction and architecture, Slovak Academy of Sciences where he is now deputy director. His main contribution belongs to the development of the Boundary element method (BEM), Regularization techniques in BEM, and Mesh-free methods. He received several fellowships from abroad (Cornell Univ., USA; Shinshu Univ., Japan; Wessex Inst. of Technol., U.K.; UCLA, USA). His research results have been recognized several times by awarding the Slovak Academy Prize, Prize of Slovak Literary Agency. He is a Fellow of the Wessex Institute, UK; member of the Editorial Board of the Series Advances in Boundary Elements (UK), Editorial Board of Boundary Element Communications, Editorial Board of Int. Jour. Eng. Analysis with Boundary Elements. He is invited into the scientific committees of international conferences and as reviewer of scientific papers from many international research journals.

Ing. Peter Staňák, born in 1985, is currently conducting his PhD. studies at Institute of Construction and Architecture, Slovak Academy of Sciences in the field of applied mechanics He finished his master's studies in the field of applied mechanics at the Faculty

of Mechanical Engineering of the Slovak Technical University in 2009. In his research and studies he focuses on application of new meshless formulations for problems of structures with incorporated smart materials.

KEY WORDS

Meshless Local Petrov-Galerkin (MLPG) Method, MLS Interpolation, Piezoelectric Solids, Transient Thermal Load, Houbolt Finite-Difference Scheme, Orthotropic Properties

ABSTRACT

In this paper meshless method based on the local Petrov-Galerkin approach is pesented for the solution of boundary value problems for coupled thermo-electro-mechanical fields. Transient dynamic governing equations are considered in analysis of the problems. Material properties of piezoelectric materials are influenced by a thermal field. It is leading to an induced nonhomogeneity and the governing equations are more complicated compared to a homogeneous counterpart. Two-dimensional analyzed domain is divided into small circular subdomains surrounding nodes that are randomly spread over the whole domain. A unit step function is used as the test functions in the local weak-form. The derived local integral equations (LIEs) have boundary-domain integral form. The moving least-squares (MLS) method is adopted for the approximation of the physical quantities in the LIEs and afterwards to obtain a system of ordinary differential equations (ODE) for unknown nodal quantities. To solve this system of ODE, Houbolt finite-difference scheme is applied as a time-stepping method.

INTRODUCTION

Many engineering applications, smart structures and devices take advantage of piezoelectric materials. Piezoelectric materials are often referred to as smart materials. They are extensively utilized as transducers, sensors and actuators in many engineering fields. Piezoelectric materials have usually anisotropic properties. Except this complication electric and mechanical fields are coupled each other and the governing equations are much more complex than those in the classical elasticity. In order to solve the boundary or the initial-boundary value problems for piezoelectric solids, efficient computational methods are required. Mostly, the finite element method (FEM) as shown in [9], [11], [13] and the boundary element method (BEM) [7], [10], [14] and [25] are applied to solve general piezoelectric problems. Meshless methods have been also successfully applied to piezoelectric problems in [16] and [20].

In certain piezoelectric materials pyroelectric effect can be observed. This means they are temperature sensitive, i.e. an electric charge or voltage is generated when exposed to temperature variations. Thus a coupling of thermo-electro-mechanical fields is needed to be taken into account if a temperature load is considered in a piezoelectric solid. Mindlin [17] for the first time introduced the theory of thermo-piezoelectricity. The physical laws for thermo-piezoelectric materials have been explored by Nowacki [19]. In the work of Dunn [8], micromechanics models for effective thermal expansion and pyroelectric coefficients of piezoelectric composites were studied. Qin [22] offered a review on fracture of thermo-piezoelectric materials. Boundary value problems for coupled fields are complex, thus analytical methods can be only applied to simple problems of thermo-piezoelectricity, e.g. [26], [27] and [32]. The analysis and design process of smart engineering structures with integrated piezoelectric actuators or sensors requires powerful calculation tools. Up to now the finite element methods (FEM) provides an effective technique, as shown in [33] in a homogeneous medium. Rao and Sunar [24] investigated the piezothermoelectric problem of intelligent structures with distributed piezoelectric sensors and actuators and concluded that the inclusion of the thermal effects may help improve the performance characteristics of the system.

Material properties under a thermal load are influenced by temperature. However, most investigations in piezothermoelasticity were done under the assumption of the temperature independent material properties. Bert and Birman [5] showed that the piezoelectric coefficients are stress and electric-field dependent. If this phenomenon is considered the material properties are continuously varying with Cartesian coordinates. In this so called induced nonhomogeneity the governing equations are more complicated than in a homogeneous counterpart. Some relative simple problems of coupled electro-mechanical fields in

continuously nonhomogeneous solids have been successfully solved in previous works [34] and [35]. Aouadi [1] made the first attempt to solve induced nonhomogeneity problem in thermo-piezoelectricity for an infinite and half-space. A general numerical solution for induced nonhomogeneity problem in thermo-piezoelectricity is not available according to the best of the author's knowledge.

The meshless local Petrov-Galerkin (MLPG) method is considered as a fundamental base for the derivation of many meshless formulations, since trial and test functions can be chosen from different functional spaces. The MLPG method introduced by Atluri et al. [2], Atluri [3] and Sladek et al. [28], using a Heaviside step function as the test functions, has been applied to solve 2-D homogeneous piezoelectric problems in paper by Sladek et al. [29].

Recently, meshless method (MLPG) was applied to analyze continuously nonhomogeneous piezoelectric solids under a mechanical or electrical load [30]. Extension of the MLPG method to 2-D thermo-piezoelectric solids with induced nonhomogeneity is given in the present paper. The coupled thermo-electro-mechanical fields in thermo-piezoelectricity are described by partial differential equations, where mechanical fields are described by the equations of motion with an inertial term. Maxwell´s equation for the electrical field has a quasi-static character and thermal field is described by the heat conduction equation, which has a diffusive character. Nodal points are introduced and spread on the analyzed domain and each node is surrounded by a small circle for simplicity, but without loss of generality. Numerical integrations over simple shape of subdomains like circles can be easily carried out. The integral equations have a very simple nonsingular form. The spatial variations of the displacements, the electric potential and the temperature are approximated by the Moving Least-Squares (MLS) scheme [4]. After performing the spatial integrations, a system of ordinary differential equations for the unknown nodal values is obtained. The boundary conditions on the global boundary are satisfied by the collocation of the MLS-approximation expressions for the displacements, the electric potential and the temperature at the boundary nodal points. Finally, the system of ordinary differential equations is solved by the Houbolt finite-difference scheme [12]. Several numerical examples are introduced to verify the accuracy and the efficiency of the proposed MLPG method.

GOVERNING EQUATIONS FOR THERMO-ELECTRO-MECHANICAL FIELDS

The governing equations for thermo-piezoelectricity in continuously nonhomogeneous solids under the quasi-electrostatic assumption are given according to Mindlin [18] by the equation of motion for displacements, the first Maxwell`s equation for the vector of electric displacements and heat conduction equation:

$$\sigma_{ij,j}(\mathbf{x},\tau) + X_i(\mathbf{x},\tau) = \rho(\mathbf{x})\ddot{u}_i(\mathbf{x},\tau) \tag{1}$$

$$D_{j,j}(\mathbf{x},\tau) - R(\mathbf{x},\tau) = 0 \tag{2}$$

$$\left[k_{ij}(\mathbf{x})\theta_{,j}(\mathbf{x},\tau)\right]_{,i} - \rho(\mathbf{x})c(\mathbf{x})\dot{\theta}(\mathbf{x},\tau) + S(\mathbf{x},\tau) = 0 \tag{3}$$

where σ_{ij}, τ, θ, u_i, D_i, X_i, R and S are stress, time, temperature difference, displacement, electric displacement, density of body force vector, volume density of free charges and density of heat sources, respectively. Adding that ρ, k_{ij} and c are the mass density, thermal conductivity tensor and specific heat, respectively. The dots over a quantity indicate the time derivatives. A static problem can be considered formally as a special case of the dynamic one, by omitting the acceleration $\ddot{u}_i(\mathbf{x},\tau)$ in the equations of motion (1) and the time derivative terms in equation (3). Both cases are analyzed here. The heat generation by mechanical and electrical fields can be neglected for most materials because the inverse thermoelastic and pyroelectric effects are very weak. Assuming this, the constitutive relations representing the partial-coupling of the mechanical, electrical and thermal fields are:

$$\sigma_{ij}(\mathbf{x},\tau) = c_{ijkl}(\mathbf{x})\varepsilon_{kl}(\mathbf{x},\tau) - e_{kij}(\mathbf{x})E_k(\mathbf{x},\tau) - \gamma_{ij}(\mathbf{x})\theta(\mathbf{x},\tau) \tag{4}$$

$$D_j(\mathbf{x},\tau) = e_{jkl}(\mathbf{x})\varepsilon_{kl}(\mathbf{x},\tau) + h_{jk}(\mathbf{x})E_k(\mathbf{x},\tau) + p_j(\mathbf{x})\theta(\mathbf{x},\tau) \tag{5}$$

where $\mathbf{c}_{ijkl}(\mathbf{x})$, $\mathbf{e}_{jkl}(\mathbf{x})$, $\mathbf{h}_{jk}(\mathbf{x})$ and $\mathbf{p}_j(\mathbf{x})$ are the elastic, piezoelectric, dielectric and pyroelectric material tensors in a continuously nonhomogeneous piezoelectric medium, respectively. The stress-temperature modulus $\boldsymbol{\gamma}_{ij}(\mathbf{x})$ can be expressed through the stiffness coefficients and the coefficients of linear thermal expansion α_{kl}

$$\gamma_{ij} = c_{ijkl}\alpha_{kl} \tag{6}$$

The strain tensor ε_{ij} and the electric field vector E_j are related to the displacements u_i and the electric potential ψ by following expressions

$$\varepsilon_{ij} = \frac{1}{2}\left(u_{i,j} + u_{j,i}\right) \tag{7}$$

$$E_j = -\psi_{,j} \tag{8}$$

Considering plane problems, the constitutive equations are frequently written in terms of the second-order tensor of elastic constants [15]. Many piezoelectric solids are transversely isotropic. Under the plane strain condition with $\varepsilon_{33}=\varepsilon_{31}=\varepsilon_{32}=E_3=0$, the constitutive equations (4) and (5) are reduced in this case to

$$\begin{bmatrix}\sigma_{11}\\ \sigma_{22}\\ \sigma_{12}\end{bmatrix} = \begin{bmatrix}c_{11} & c_{12} & 0\\ c_{12} & c_{22} & 0\\ 0 & 0 & c_{66}\end{bmatrix}\begin{bmatrix}\varepsilon_{11}\\ \varepsilon_{22}\\ 2\varepsilon_{12}\end{bmatrix} - \begin{bmatrix}0 & e_{21}\\ 0 & e_{22}\\ e_{15} & 0\end{bmatrix}\begin{bmatrix}E_1\\ E_2\end{bmatrix} -$$

$$-\boldsymbol{\gamma}\theta = \mathbf{C}(\mathbf{x})\begin{bmatrix}\varepsilon_{11}\\ \varepsilon_{22}\\ 2\varepsilon_{12}\end{bmatrix} - \mathbf{L}(\mathbf{x})\begin{bmatrix}E_1\\ E_2\end{bmatrix} - \boldsymbol{\gamma}\theta \tag{9}$$

$$\begin{bmatrix}D_1\\ D_2\end{bmatrix} = \begin{bmatrix}0 & 0 & e_{15}\\ e_{21} & e_{22} & 0\end{bmatrix}\begin{bmatrix}\varepsilon_{11}\\ \varepsilon_{22}\\ 2\varepsilon_{12}\end{bmatrix} + \begin{bmatrix}h_{11} & 0\\ 0 & h_{22}\end{bmatrix}\begin{bmatrix}E_1\\ E_2\end{bmatrix} +$$

$$+\begin{bmatrix}p_1\\ p_2\end{bmatrix}\theta = \mathbf{G}(\mathbf{x})\begin{bmatrix}\varepsilon_{11}\\ \varepsilon_{22}\\ 2\varepsilon_{12}\end{bmatrix} + \mathbf{H}(\mathbf{x})\begin{bmatrix}E_1\\ E_2\end{bmatrix} + \mathbf{P}(\mathbf{x})\theta \tag{10}$$

where

$$\boldsymbol{\gamma} = \begin{bmatrix}c_{11} & c_{12} & c_{13}\\ c_{12} & c_{22} & c_{23}\\ 0 & 0 & 0\end{bmatrix}\begin{bmatrix}\alpha_{11}\\ \alpha_{22}\\ \alpha_{33}\end{bmatrix} = \begin{bmatrix}\gamma_{11}\\ \gamma_{22}\\ 0\end{bmatrix}$$

For the mechanical field following essential and natural boundary conditions are assumed:

$$u_i(\mathbf{x},\tau) = \tilde{u}_i(\mathbf{x},\tau)\,\text{on}\,\Gamma_u,$$
$$t_i(\mathbf{x},\tau) = \sigma_{ij}n_j = \tilde{t}_i(\mathbf{x},\tau)\,\text{on}\,\Gamma_t,$$

for the electrical field:

$$\psi(\mathbf{x}) = \tilde{\psi}(\mathbf{x})\,\text{on}\,\Gamma_p,\; n_i D_i(\mathbf{x}) = \tilde{Q}(\mathbf{x})\,\text{on}\,\Gamma_q,$$

and finally for the thermal field:

$$\theta(\mathbf{x},\tau) = \tilde{\theta}(\mathbf{x},\tau)\,\text{on}\,\Gamma_a,$$
$$q(\mathbf{x},\tau) = k_{ij}\theta_{,j}(\mathbf{x},\tau)n_i(\mathbf{x}) = \tilde{q}(\mathbf{x},\tau)\,\text{on}\,\Gamma_b$$

where Γ_u is the part of the global boundary with prescribed displacements, and on Γ_t, Γ_p, Γ_q, Γ_a, and Γ_b the traction vector, the electric potential, the surface charge density, the temperature and the heat flux are prescribed, respectively.

FORMULATION OF LOCAL INTEGRAL EQUATIONS

The MLPG method is applied to construct a weak-form over the local fictitious subdomains Ω_s, which is a small region taken for each node inside the global domain, as shown in [3]. The local subdomains overlap each other, and cover the whole global domain Ω. The local subdomains could be of any geometrical shape and size. In the present paper, the local subdomains are considered to be of the circular shape. The local weak-form of the governing equation (1) can be written as

$$\int_{\Omega_s}\left[\sigma_{ij,j}(\mathbf{x},\tau) - \rho(\mathbf{x})\ddot{u}_i(\mathbf{x},\tau) + X_i(\mathbf{x},\tau)\right]u_{ik}^*(\mathbf{x})\,d\Omega = 0 \tag{11}$$

where $u_{ik}^*(\mathbf{x})$ is a test function.
Applying the Gauss divergence theorem to eq. (11) and rearranging, one can obtain

$$\int_{\partial\Omega_s}\sigma_{ij}(\mathbf{x},\tau)n_j(\mathbf{x})u_{ik}^*(\mathbf{x})d\Gamma - \int_{\Omega_s}\sigma_{ij}(\mathbf{x},\tau)u_{ik,j}^*(\mathbf{x})d\Omega + \int_{\Omega_s}\left[X_i(\mathbf{x},\tau) - \rho(\mathbf{x})\ddot{u}_i(\mathbf{x},\tau)\right]u_{ik}^*(\mathbf{x})d\Omega = 0 \tag{12}$$

where $\partial\Omega_s$ is the boundary of the local subdomain which consists of three parts $\partial\Omega_s = L_s \cup \Gamma_{st} \cup \Gamma_{su}$ [3]. Here L_s is the local boundary that is totally inside the

global domain, Γ_{st} is the part of the local boundary which coincides with the global traction boundary, i.e., $\Gamma_{st} = \partial\Omega_s \cap \Gamma_t$ and similarly Γ_{su} is the part of the local boundary that coincides with the global displacement boundary, i.e. $\Gamma_{su} = \partial\Omega_s \cap \Gamma_u$.
Heaviside step function is chosen as the test function $u_{ik}^{*}(\mathbf{x})$ in each subdomain

$$u_{ik}^{*}(\mathbf{x}) = \begin{cases} \delta_{ik} & \text{at} \quad \mathbf{x} \in \Omega_s \\ 0 & \text{at} \quad \mathbf{x} \notin \Omega_s \end{cases}$$

and using this, the local weak-form (12) is converted into the following local boundary-domain equations

$$\int_{L_s+\Gamma_{su}} t_i(\mathbf{x},\tau)d\Gamma - \int_{\Omega_s} \rho(\mathbf{x})\ddot{u}_i(\mathbf{x},\tau)d\Omega = \\ = -\int_{\Gamma_{st}} \tilde{t}_i(\mathbf{x},\tau)d\Gamma - \int_{\Omega_s} X_i(\mathbf{x},\tau)d\Omega \qquad (13)$$

It is important to note that the local integral equations (13) are valid for both homogeneous and non-homogeneous linear piezoelelectric solids. Nonhomogeneous material properties are included in eq. (13) through the elastic and piezoelectric tensor of the material coefficients in the traction components.
The local weak form of the governing equation (2) is given in the similar way as

$$\int_{\Omega_s} \left[D_{j,j}(\mathbf{x},\tau) - R(\mathbf{x},\tau) \right] v^{*}(\mathbf{x})\, d\Omega \;\; = 0 \qquad (14)$$

where $v^{*}(\mathbf{x})$ is a test function.
Again, as in previous case, applying the Gauss divergence theorem to the local weak-form (14) and considering the Heaviside step function for the test function $v^{*}(\mathbf{x})$, one will obtain

$$\int_{L_s+\Gamma_{sp}} Q(\mathbf{x},\tau)d\Gamma = -\int_{\Gamma_{sq}} \tilde{Q}(\mathbf{x},\tau)d\Gamma + \int_{\Omega_s} R(\mathbf{x},\tau)d\Omega \qquad (15)$$

where $Q(\mathbf{x},\tau) = D_j(\mathbf{x},\tau)n_j$.
The local weak-form of the diffusion equation (3) can be written as

$$\int_{\Omega_s} \left\{ \left[k_{ij}(\mathbf{x})\theta_{,j}(\mathbf{x},\tau) \right]_{,i} - \rho(\mathbf{x})c(\mathbf{x})\dot{\theta}(\mathbf{x},\tau) + \right. \\ \left. + W(\mathbf{x},\tau) \right\} w^{*}(\mathbf{x})\, d\Omega = 0 \qquad (16)$$

where $w^{*}(\mathbf{x})$ is a test function.
Applying the Gauss divergence theorem to the local weak-form (16) and considering the Heaviside step function for the test function $w^{*}(\mathbf{x})$ one can obtain

$$\int_{L_s+\Gam_{sa}} q(\mathbf{x},\tau)d\Gamma - \int_{\Omega_s} \rho(\mathbf{x})c(\mathbf{x})\dot{\theta}(\mathbf{x},\tau)d\Omega = \\ = -\int_{\Gamma_{sb}} q(\mathbf{x},\tau)d\Gamma - \int_{\Omega_s} S(\mathbf{x},\tau)d\Omega \qquad (17)$$

There is no requirement in the MLPG method on the test and the trial functions to be necessarily from the same functional spaces. For internal nodes, the test function is chosen as the Heaviside step function with its support on the local subdomain. The trial functions, on the other hand, are chosen to be the moving least-squares (MLS) approximation over a number of nodes spread within the domain of influence. The approximated functions for the mechanical displacements, the electric potential and the temperature can be written according to Atluri [4] as:

$$\mathrm{u}^{h}(\mathbf{x},\tau) = \Phi^{T}(\mathbf{x}) \cdot \hat{\mathbf{u}}(\tau) = \sum_{a=1}^{n} \phi^{a}(\mathbf{x})\, \hat{\mathbf{u}}^{a}(\tau)$$

$$\psi^{h}(\mathbf{x},\tau) = \sum_{a=1}^{n} \phi^{a}(\mathbf{x})\hat{\psi}^{a}(\tau)$$

$$\theta^{h}(\mathbf{x},\tau) = \sum_{a=1}^{n} \phi^{a}(\mathbf{x})\hat{\theta}^{a}(\tau) \qquad (18)$$

where the nodal values $\hat{\mathrm{u}}^{a}(\tau)$, $\hat{\psi}^{a}(\tau)$ and $\hat{\theta}^{a}(\tau)$ are fictitious parameters for the displacements, the electric potential and the temperature, respectively, and $\phi^{a}(\mathbf{x})$ is the shape function associated with the node a. The number of nodes n used for the approximation is determined by the weight function $w^{a}(\mathbf{x})$. In the MLS approximation a 4th order spline-type weight function is applied [3]. It can be easily shown, that the C^{1} - continuity is ensured over the entire domain, therefore the continuity conditions of the tractions, the electric charge and the heat flux will be satisfied.
The traction vector $t_i(\mathbf{x},\tau)$ at a boundary point $\mathbf{x} \in \partial\Omega_S$ is approximated in terms of the same nodal values $\hat{\mathrm{u}}^{a}(\tau)$ as

$$\mathbf{t}^{h}(\mathbf{x},\tau) = \mathbf{N}(\mathbf{x})\mathbf{C}(\mathbf{x})\sum_{a=1}^{n} \mathbf{B}^{a}(\mathbf{x})\hat{\mathbf{u}}^{a}(\tau) \;\; +$$

$$+\mathbf{N}(\mathbf{x})\mathbf{L}(\mathbf{x})\sum_{a=1}^{n}\mathbf{A}^{a}(\mathbf{x})\hat{\psi}^{a}(\tau)-$$

$$-\mathbf{N}(\mathbf{x})\boldsymbol{\gamma}\sum_{a=1}^{n}\phi^{a}(\mathbf{x})\hat{\theta}^{a}(\tau) \qquad (19)$$

where the matrix $\mathbf{N}(\mathbf{x})$ is related to the normal vector $\mathbf{n}(\mathbf{x})$ on $\partial\Omega_S$ by

$$\mathbf{N}(\mathbf{x})=\begin{bmatrix} n_1 & 0 & n_2 \\ 0 & n_2 & n_1 \end{bmatrix}$$

and the matrices $\mathbf{B}^a$ and $\mathbf{A}^a$ are represented by the gradients of the shape functions as

$$\mathbf{B}^{a}(\mathbf{x})=\begin{bmatrix} \phi^{a}_{,1} & 0 \\ 0 & \phi^{a}_{,2} \\ \phi^{a}_{,2} & \phi^{a}_{,1} \end{bmatrix}, \mathbf{A}^{a}(\mathbf{x})=\begin{bmatrix} \phi^{a}_{,1} \\ \phi^{a}_{,2} \end{bmatrix}$$

The electrical charge $Q(\mathbf{x},\tau)$ can be approximated in similar way by

$$Q^{h}(\mathbf{x},\tau)=\mathbf{N}_1(\mathbf{x})\mathbf{G}(\mathbf{x})\sum_{a=1}^{n}\mathbf{B}^{a}(\mathbf{x})\hat{\mathbf{u}}^{a}(\tau) \; -$$

$$-\mathbf{N}_1(\mathbf{x})\mathbf{H}(\mathbf{x})\sum_{a=1}^{n}\mathbf{A}^{a}(\mathbf{x})\hat{\psi}^{a}(\tau)+$$

$$+\mathbf{N}_1(\mathbf{x})\mathbf{P}(\mathbf{x})\sum_{a=1}^{n}\phi^{a}(\mathbf{x})\hat{\theta}^{a}(\tau) \qquad (20)$$

where the matrices $\mathbf{G}$ and $\mathbf{H}$ are defined in eq. (10) and $\mathbf{N}_1(\mathbf{x})=[n_1 \;\; n_2]$.
The heat flux $q(\mathbf{x},\tau)$ is approximated by

$$q^{h}(\mathbf{x},\tau)=k_{ij}n_i\sum_{a=1}^{n}\phi^{a}_{,j}(\mathbf{x})\hat{\theta}^{a}(\tau)=$$

$$=\mathbf{N}_1(\mathbf{x})\mathbf{K}(\mathbf{x})\sum_{a=1}^{n}\mathbf{A}^{a}(\mathbf{x})\hat{\theta}^{a}(\tau) \qquad (21)$$

where

$$\mathbf{K}(\mathbf{x})=\begin{bmatrix} k_{11} & k_{12} \\ k_{12} & k_{22} \end{bmatrix}$$

Using the approximation formula (18) and fulfilling the essential boundary conditions at those nodal points on the global boundary, where the displacements, the electrical potential and the temperature are prescribed, discretized form of the boundary conditions is obtained as

$$\sum_{a=1}^{n}\phi^{a}(\zeta)\hat{\mathbf{u}}^{a}(\tau)=\tilde{\mathbf{u}}(\zeta,\tau)\,\text{for}\,\zeta\in\Gamma_u \qquad (22)$$

$$\sum_{a=1}^{n}\phi^{a}(\zeta)\hat{\boldsymbol{\psi}}^{a}(\tau)=\tilde{\boldsymbol{\psi}}(\zeta,\tau)\,\text{for}\,\zeta\in\Gamma_p \qquad (23)$$

$$\sum_{a=1}^{n}\phi^{a}(\zeta)\hat{\boldsymbol{\theta}}^{a}(\tau)=\tilde{\boldsymbol{\theta}}(\zeta,\tau)\,\text{for}\,\zeta\in\Gamma_a \qquad (24)$$

Discretized forms of the unknown quantities in the local boundary-domain integral equations (13), (15) and (17) are obtained in the view of the MLS-approximation (19) - (21) as

$$\sum_{a=1}^{n}\left(\int_{L_s+\Gamma_{su}}\mathbf{N}(\mathbf{x})\mathbf{C}(\mathbf{x})\mathbf{B}^{a}(\mathbf{x})d\Gamma\right)\hat{\mathbf{u}}^{a}(\tau)-$$

$$-\sum_{a=1}^{n}\rho\left(\int_{\Omega_s}\phi^{a}(\mathbf{x})d\Omega\right)\ddot{\hat{\mathbf{u}}}^{a}(\tau)+$$

$$+\sum_{a=1}^{n}\left(\int_{L_s+\Gamma_{su}}\mathbf{N}(\mathbf{x})\mathbf{L}(\mathbf{x})\mathbf{A}^{a}(\mathbf{x})d\Gamma\right)\hat{\psi}^{a}(\tau) \; -$$

$$-\sum_{a=1}^{n}\left(\int_{L_s+\Gamma_{su}}\mathbf{N}(\mathbf{x})\boldsymbol{\gamma}(\mathbf{x})\phi^{a}(\mathbf{x})d\Gamma\right)\hat{\theta}^{a}(\tau)=$$

$$=-\int_{\Gamma_{st}}\tilde{\mathbf{t}}(\mathbf{x},\tau)d\Gamma-\int_{\Omega_s}\mathbf{X}(\mathbf{x},\tau)d\Omega \qquad (25)$$

$$\sum_{a=1}^{n}\left(\int_{L_s+\Gamma_{sp}}\mathbf{N}_1(\mathbf{x})\mathbf{G}(\mathbf{x})\mathbf{B}^{a}(\mathbf{x})d\Gamma\right)\hat{\mathbf{u}}^{a}(\tau) \; -$$

$$-\sum_{a=1}^{n}\left(\int_{L_s+\Gamma_{sp}}\mathbf{N}_1(\mathbf{x})\mathbf{H}(\mathbf{x})\mathbf{A}^{a}(\mathbf{x})d\Gamma\right)\hat{\psi}^{a}(\tau)+$$

$$+\sum_{a=1}^{n}\left(\int_{L_s+\Gamma_{sp}}\mathbf{N}_1(\mathbf{x})\mathbf{P}(\mathbf{x})\phi^{a}(\mathbf{x})d\Gamma\right)\hat{\theta}^{a}(\tau)=$$

$$=-\int_{\Gamma_{sq}}\tilde{Q}(\mathbf{x},\tau)d\Gamma+\int_{\Omega_s}R(\mathbf{x},\tau)d\Omega \qquad (26)$$

$$\sum_{a=1}^{n}\left(\int_{L_s+\Gamma_{sa}}\mathbf{N}_1(\mathbf{x})\mathbf{K}(\mathbf{x})\mathbf{A}^{a}(\mathbf{x})d\Gamma\right)\hat{\theta}^{a}(\tau)-$$

$$-\sum_{a=1}^{n}\rho\left(\int_{\Omega_s}c\phi^{a}(\mathbf{x})d\Gamma\right)\dot{\hat{\theta}}^{a}(\tau)=$$

$$=-\int_{\Gamma_{sb}}\tilde{q}(\mathbf{x},\tau)d\Gamma-\int_{\Omega_s}S(\mathbf{x},\tau)d\Omega \qquad (27)$$

Equations (25), (26) and (27) are considered on the sub-domains adjacent to interior nodes as well as to the boundary nodes on Γ_{st}, Γ_{sq} and Γ_{sb}.

Complete system of ordinary differential equations for the computation of the nodal unknowns can be obtained by collecting the discretized local boundary-domain integral equations together with the discretized boundary conditions for the displacements, the electrical potential and the temperature. As nodal unknowns the fictitious parameters $\hat{\mathbf{u}}^a(\tau)$, $\hat{\psi}^a(\tau)$ and $\hat{\theta}^a(\tau)$ are considered.

General variation of material properties with Cartesian coordinates was assumed in previous formulations. If material parameters are dependent on temperature, one can write for a general material parameter A:

$$A(\mathbf{x}) = f(\theta(\mathbf{x})) \tag{28}$$

Using equation (28) to replace material parameters in constitutive equations (4) and (5), a nonlinear expression is obtained. This results in necessity of application of iterative approach in each time step. The linearized constitutive equations in the k-th iteration step are then given as

$$\begin{aligned}&\sigma_{ij}^{(k)}(\mathbf{x},\tau) = c_{ijkl}^{(k-1)}(\theta)\varepsilon_{kl}^{(k)}(\mathbf{x},\tau) - \\ &-e_{kij}^{(k-1)}(\theta)E_k^{(k)}(\mathbf{x},\tau) - \gamma_{ij}^{(k-1)}(\theta)\theta^{(k)}(\mathbf{x},\tau)\end{aligned} \tag{29}$$

$$\begin{aligned}&D_j^{(k)}(\mathbf{x},\tau) = e_{jkl}^{(k-1)}(\theta)\varepsilon_{kl}^{(k)}(\mathbf{x},\tau) + \\ &+h_{jk}^{(k-1)}(\theta)E_k^{(k)}(\mathbf{x},\tau) + p_j^{(k-1)}(\theta)\theta^{(k)}(\mathbf{x},\tau)\end{aligned} \tag{30}$$

Applying now equations (29) and (30) stated above, we obtain a set of ordinary differential equations for the k-th iteration step in form

$$\begin{aligned}&\sum_{a=1}^{n}\left(\int_{L_s+\Gamma_{su}}\mathbf{N}(\mathbf{x})\mathbf{C}^{(k-1)}(\mathbf{x})\mathbf{B}^a(\mathbf{x})d\Gamma\right)\hat{\mathbf{u}}^{a(k)}(\tau) - \\ &-\sum_{a=1}^{n}\rho(\mathbf{x})\left(\int_{\Omega_s}\phi^a(\mathbf{x})d\Omega\right)\ddot{\hat{\mathbf{u}}}^{a(k)}(\tau) + \\ &+\sum_{a=1}^{n}\left(\int_{L_s+\Gamma_{su}}\mathbf{N}(\mathbf{x})\mathbf{L}^{(k-1)}(\mathbf{x})\mathbf{A}^a(\mathbf{x})d\Gamma\right)\hat{\psi}^{a(k)}(\tau) - \\ &-\sum_{a=1}^{n}\left(\int_{L_s+\Gamma_{su}}\mathbf{N}(\mathbf{x})\boldsymbol{\gamma}^{(k-1)}(\mathbf{x})\phi^a(\mathbf{x})d\Gamma\right)\hat{\theta}^{a(k)}(\tau) = \\ &=-\int_{\Gamma_{st}}\tilde{\mathbf{t}}(\mathbf{x},\tau)d\Gamma - \int_{\Omega_s}\mathbf{X}(\mathbf{x},\tau)d\Omega\end{aligned} \tag{31}$$

$$\begin{aligned}&\sum_{a=1}^{n}\left(\int_{L_s+\Gamma_{sp}}\mathbf{N}_1(\mathbf{x})\mathbf{G}^{(k-1)}(\mathbf{x})\mathbf{B}^a(\mathbf{x})d\Gamma\right)\hat{\mathbf{u}}^{a(k)}(\tau) - \\ &-\sum_{a=1}^{n}\left(\int_{L_s+\Gamma_{sp}}\mathbf{N}_1(\mathbf{x})\mathbf{H}^{(k-1)}(\mathbf{x})\mathbf{A}^a(\mathbf{x})d\Gamma\right)\hat{\psi}^{a(k)}(\tau) + \\ &+\sum_{a=1}^{n}\left(\int_{L_s+\Gamma_{sp}}\mathbf{N}_1(\mathbf{x})\mathbf{P}^{(k-1)}(\mathbf{x})\phi^a(\mathbf{x})d\Gamma\right)\hat{\theta}^{a(k)}(\tau) = \\ &=-\int_{\Gamma_{sq}}\tilde{Q}(\mathbf{x},\tau)d\Gamma + \int_{\Omega_s}R(\mathbf{x},\tau)d\Omega\end{aligned} \tag{32}$$

$$\begin{aligned}&\sum_{a=1}^{n}\left(\int_{L_s+\Gamma_{sa}}\mathbf{N}_1(\mathbf{x})\mathbf{K}^{(k-1)}(\mathbf{x})\mathbf{A}^a(\mathbf{x})d\Gamma\right)\dot{\hat{\theta}}^{a(k)}(\tau) - \\ &-\sum_{a=1}^{n}\rho(\mathbf{x})\left(\int_{\Omega_s}c(\mathbf{x})\phi^a(\mathbf{x})d\Gamma\right)\hat{\theta}^{a(k)}(\tau) = \\ &=-\int_{\Gamma_{sb}}\tilde{q}(\mathbf{x},\tau)d\Gamma - \int_{\Omega_s}S(\mathbf{x},\tau)d\Omega\end{aligned} \tag{33}$$

Material parameters are taken at a reference temperature for the 1st iteration step. The iteration process is ended if the difference of the Sobolev-norms for temperatures in two successive steps is smaller than a prescribed tolerance.

Now, we should explain solution of the complete system of ordinary differential equations. The system of above given local integral equations can be rearranged in such a way that all known quantities are on the r.h.s. Thus, in matrix form the system becomes

$$\mathbf{A}\ddot{\mathbf{x}} + \mathbf{B}\dot{\mathbf{x}} + \mathbf{C}\mathbf{x} = \mathbf{Y} \tag{34}$$

In the present work, the Houbolt method is applied. In the Houbolt finite-difference scheme [12], the "acceleration" ($\ddot{\mathbf{u}}=\ddot{\mathbf{x}}$) is expressed as

$$\ddot{\mathbf{x}}_{\tau+\Delta\tau} = \frac{2\mathbf{x}_{\tau+\Delta\tau} - 5\mathbf{x}_{\tau} + 4\mathbf{x}_{\tau-\Delta\tau} - \mathbf{x}_{\tau-2\Delta\tau}}{\Delta\tau^2} \tag{35}$$

where $\Delta\tau$ is the time step. The backward difference method is applied for the approximation of "velocities"

$$\dot{\mathbf{x}}_{\tau+\Delta\tau} = \frac{\mathbf{x}_{\tau+\Delta\tau} - \mathbf{x}_{\tau}}{\Delta\tau} \tag{36}$$

Substituting eqs. (35) and (36) into eq. (34), we get

the following system of algebraic equations for the unknowns $\mathbf{x}_{\tau+\Delta\tau}$

$$\left[\frac{2}{\Delta\tau^2}\mathbf{A}+\frac{1}{\Delta\tau}\mathbf{B}+\mathbf{C}\right]\mathbf{x}_{\tau+\Delta\tau}=\frac{1}{\Delta\tau^2}(5\mathbf{A}+\mathbf{B}\Delta\tau)\mathbf{x}_{\tau}+$$
$$+\mathbf{A}\frac{1}{\Delta\tau^2}\{-4\mathbf{x}_{\tau-\Delta\tau}+\mathbf{x}_{\tau-2\Delta\tau}\}+\mathbf{Y} \qquad (37)$$

The value of the time step has to be appropriately selected with respect to material parameters (wave velocities) and time dependence of the boundary conditions.

NUMERICAL EXAMPLES

Numerical results are presented in this section for selected problems of thermoelasticity in piezoelectric materials.

In order to test the accuracy of the present meshless method a unit square panel under a sudden heating on the top side is analyzed as the first example (Fig. 1). The following analytical solution is available for uncoupled thermoelasticity in an isotropic material [6]:

$$\theta(x_2,\tau)=1-\frac{4}{\pi}\sum_{n=0}^{\infty}\left\{\frac{(-1)^n}{2n+1}\exp\left[-\frac{(2n+1)^2\pi^2\kappa\tau}{4a^2}\right]\right.$$
$$\left.\cos\left(\frac{(2n+1)\pi x_2}{2a}\right)\right\} \qquad (38)$$

where a is the side-length of the panel and $\kappa=k_{22}/\rho c$ is the diffusivity coefficient.

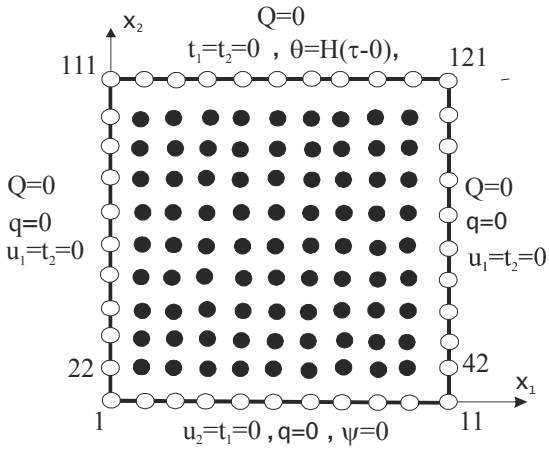

Fig. 1 *Uniformly heated piezoelectric square plate*

Homogeneous material properties are selected to test the present computational method. The material coefficients of the panel are considered for PZT-5H according to Qin and Mai [23]:
$c_{11}=12{,}6.10^{10}\mathrm{Nm}^{-2}$, $c_{12}=5{,}3.10^{10}\mathrm{Nm}^{-2}$,
$c_{22}=11{,}7.10^{10}\mathrm{Nm}^{-2}$, $c_{44}=3{,}53.10^{10}\mathrm{Nm}^{-2}$,
$e_{15}=17\mathrm{Cm}^{-2}$, $e_{21}=-6{,}5\mathrm{Cm}^{-2}$, $e_{22}=23{,}3\mathrm{Cm}^{-2}$,
$h_{11}=15{,}1.10^{-9}\mathrm{C(Vm)}^{-1}$, $h_{22}=13.10^{-9}\mathrm{C(Vm)}^{-1}$,
$\rho=7500\mathrm{kg/m}^3$, $k_{11}=50\mathrm{W/Km}$,
$k_{22}=75\mathrm{W/Km}$, $\alpha_{11}=0{,}88.10^{-5}1/\mathrm{K}$,
$\alpha_{22}=0{,}5.10^{-5}1/\mathrm{K}$, $p_1=0$,
$p_2=-5{,}4831.10^{-6}\mathrm{C/Km}^2$, $c=420\mathrm{Wskg}^{-1}\mathrm{K}^{-1}$.

Plane strain condition is assumed in the analysis. The mechanical displacement, the electrical potential and the thermal field on the finite square panel with a size $a \times a=1\mathrm{m} \times 1\mathrm{m}$ are approximated by using 121 (11×11) equaly-spaced nodes. The circular local sub-domains are considered, each with a radius $r_{loc}=0{,}08$. The Sobolev-norm is calculated for the purpose of error analysis. The relative error of the temperature in the considered time interval $[0,T]$ is defined as

$$r=\frac{\left\|\theta^{num}-\theta^{exact}\right\|}{\left\|\theta^{exact}\right\|} \qquad (39)$$

where

$$\|\theta\|=\left(\int_0^T\theta^2 d\tau\right)^{1/2}$$

and time T is defined through normalized parameter $Tk_{22}/\rho ca^2=1{,}3$.

Fig. 2 presents numerical results for the temperature at the bottom side and the mid-line of the panel. The temperature is normalized by the intensity of the thermal shock $\theta_0=0$. Obtained results are compared with the analytical results and an excellent agreement is observed. The relative error of the temperature, r, at both lines is less than 0,5%. For the total number of 441 nodes, the relative error $r=0{,}15\%$ has been obtained. The temperature distribution is not influenced by mechanical and electrical fields.

Numerical results for the temporal variation of the direct stress σ_{11} are presented in Fig. 3, an excellent agreement can be seen again between the presented and FEM results computed at both considered lines. The FEM results have been obtained by ANSYS code with 3600 quadratic eight-node elements and 1000 time increments. The stresses are normalized

by the static value σ_{11}^{stat} =-1,2959.10^{6}Pa.

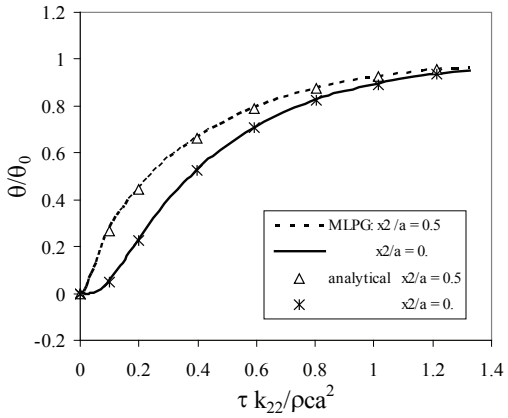

Fig. 2 *Time variation of the temperature on two different lines parallel to* x_1*- axis*

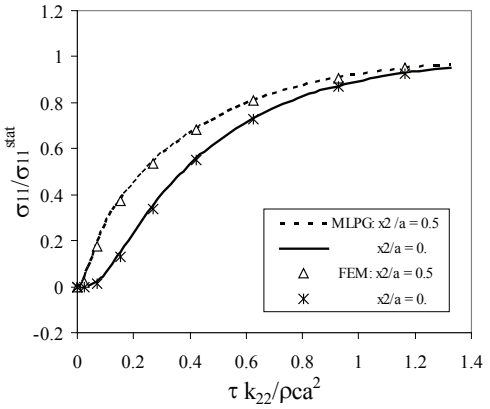

Fig. 3 *Time variation of the* σ_{11} *stress*

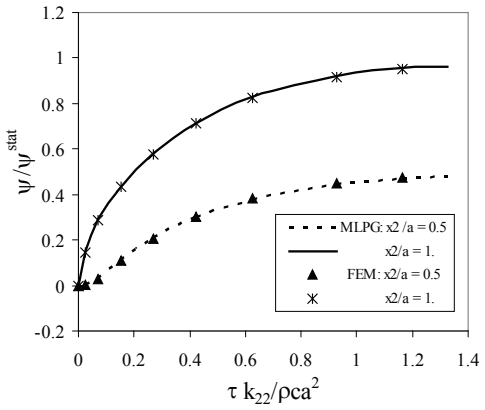

Fig. 4 *Time variation of the electric potential at two different lines parallel to* x_1*- axis*

The temporal variation of the electrical potential Ψ is shown in Fig. 4. The potential is normalized by the static value Ψ^{stat}=1,4861.10^{4}V at the top side of the panel if the pyroelectric material vector $\mathbf{P}^T=(p_1,p_2)$ is vanishing. For p_2=−5,4831.10^{-6}C/Km^2 we have obtained the static value Ψ^{stat}=1,455.10^{4}V. One can observe that the pyroeletric parameter is only slightly decreasing the electrical potential in the considered problem.

In order to control the mechanical quantities (displacements and stresses) the inverse piezoelectric effect can be utilized. So as a next load case, we have applied a uniform electrical displacement D_0 on the top side of the panel additionally to the thermal load. Stationary boundary conditions are considered. In Fig. 5 one can observe the influence of the electrical displacement on the stress component σ_{11}. The increasing electrical displacement on the top side of the panel significantly reduces the normal stress. The electrical displacement is expressed through the normalized quantity $\lambda = D_0 e_{22} / h_{22} c_{11} \alpha_{11} \theta_0$. Negligible influence of the pyroelectric parameters on the stress values can be observed.

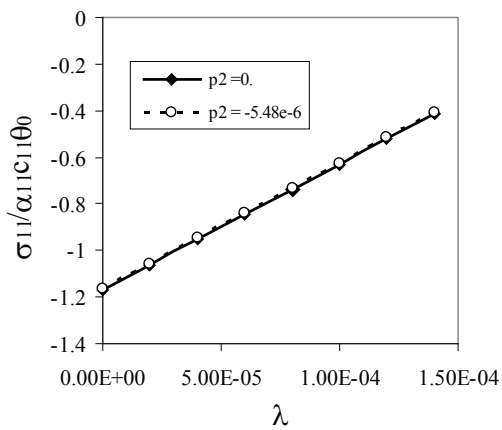

Fig. 5 *Variation of the* σ_{11} *stress with the normalized electrical displacements*

As the next example, an edge crack in a finite piezoelectric strip is analyzed. The geometry of the strip is given in Fig. 6 with the following values: a=*0,5m*, a/w=*0,4* and h/w=*1,2*. Only a half of the strip is modeled due to the symmetry of the problem with respect to the x_1 - axis. We have used 930 nodes equidistantly distributed for the MLS approximation of the physical quantities. On the both lateral sides of the strip thermal load is applied.

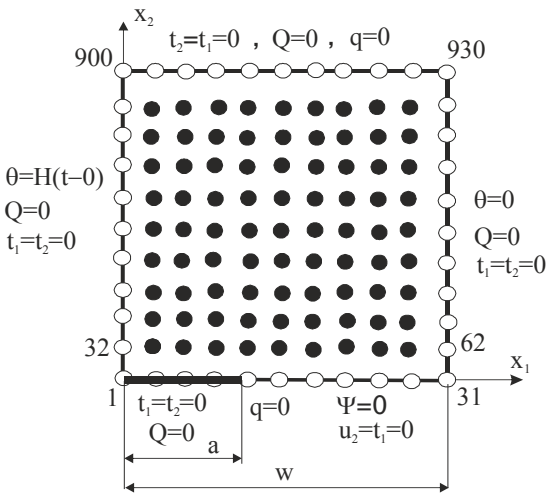

Fig. 6 *Edge crack in a finite strip under a thermal shock, half of the strip depicted due to a symmetry*

For cracks in homogeneous and linear piezoelectric solids the asymptotic behaviour of the field quantities has been given by Sosa [31] and Pak [21]. Using these expressions, one can obtain the following expression for the intensity factors [10] as

$$\begin{pmatrix} K_I \\ K_{IV} \end{pmatrix} = \lim_{r\to 0} \sqrt{\frac{\pi}{8r}} \left[\mathrm{Re}(\mathbf{B})^{-1} \right] \begin{pmatrix} \Delta u_2 \\ \Delta \psi \end{pmatrix} \qquad (40)$$

where the matrix **B** is determined by the material properties in paper by Garcia-Sanchez et al. [10]. Note that the symmetry conditions of the displacements and the potential with respect to the crack plane are utilized.

Contrary to the static case, the SIF is not vanishing for the thermal shock prescribed on the left lateral side of the strip. From the Maxwell`s equations, it is known that the velocity of electromagnetic waves is equal to the speed of light, which is much greater than the velocity of elastic and thermal waves. Hence, the use of quasi-static approximation in eqs. (1) to (3) is justified for the interaction of electrical, mechanical and thermal fields. The response of the electric fields is immediate, while that of the elastic and thermal ones are taken as finite because of the finite velocity of both waves. On the other hand, in a static case, the response of all the mechanical (strain, stress), thermal and electrical fields is immediate. Thus, the SIF is vanishing in such a case since the stresses are zero ahead the crack-tip on the crack line because of the immediate electro-mechanical interaction. In the dynamic case the stress field is coupled not only to the immediate electric field, but also to inertia forces [9]. Numerical results for the normalized stress intensity factor $fI=KI/\sqrt{\pi a}\ \alpha_{11}c_{11}\theta_0$ are presented in Fig. 7. On the right lateral side of the finite specimen a vanishing heat flux is considered in the transient heat conduction case. We have also considered an induced nonhomogeneity caused by the dependence of the thermal expansion coefficient on the temperature, $\alpha_{kl}= \alpha_{kl0}(1-\mathrm{m}\theta)$, where $\mathrm{m}=0{,}005K^{-1}$. It can be well observed that for a large time instant the SIF is vanishing in Fig. 7. The electrical displacement intensity factor (EDIF) for considered boundary value problem is vanishing since the thermal processes changes are relatively slow.

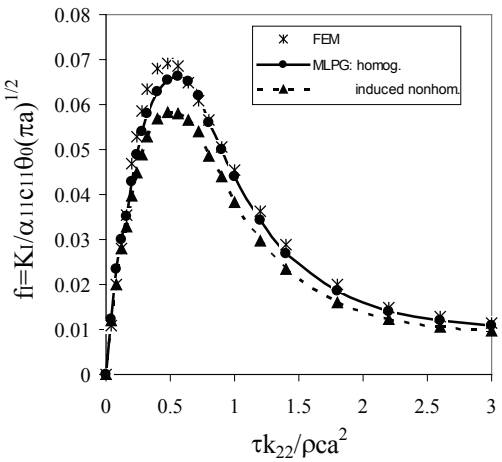

Fig. 7 *Time variation of the stress intensity factor for an edge crack*

CONCLUSION

A meshless local Petrov-Galerkin method (MLPG) is proposed for the solution of boundary value problems for coupled thermo-electro-mechanical fields. Transient dynamic governing equations are considered. The material properties of a piezoelectric material are influenced by a thermal field. It is leading to an induced nonhomogeneity and so to mathematical complications of the governing equations compared to a homogeneous counterpart. The analyzed domain is divided into small overlapping circular subdomains. A unit step function is used as the test functions in the local weak-form of the governing partial differential equations. For the approxi-

mation of the physical field quantities the Moving Least-Squares (MLS) scheme is used. The proposed method is a truly meshless method, which requires neither domain elements nor background cells in either the interpolation or the integration.

The present method represents an alternative numerical tool for many existing computational methods like the FEM or the BEM. The main advantage of the present method is its simplicity. The present formulation is promising for numerical analyses of multi-field problems like piezoelectric or thermoelastic problems.

ACKNOWLEDGEMENT

The authors gratefully acknowledge the support by the Slovak Science and Technology Assistance Agency registered under number APVV-0427-07 and the Slovak Grant Agency VEGA-2/0039/09.

REFERENCES

[1] Aouadi M., Generalized thermo-piezoelectric problems with temperature-dependent properties, Int. J. Solids Structures, vol. 43, 2006, p. 6347-6358

[2] Ashida F., Tauchert T.R., Noda N., Potential function method for piezothermoelastic problems of solids of crystal class 6 mm in cylindrical coordinates, Journal of Thermal Stresses, vol. 17, 1994, p. 361-375

[3] Atluri S.N., The Meshless Method (MLPG) for Domain & BIE Discretizations, Tech Science Press, Forsyth, GA, USA, 2004

[4] Belytschko T., Krogauz Y., Organ D., Fleming M., Krysl P., Meshless methods; an overview and recent developments, Comp. Meth. Appl. Mech. Engn., vol. 139, 1996, p. 3-47

[5] Bert C.W., Birman, V., Stress dependency of the thermoelastic and piezoelectric coefficients, AIAA Journal, vol. 37, 1999, p. 135-137

[6] Carslaw H.S., Jaeger J.C., Conduction of Heat in Solids, Clarendon, Oxford, 1959

[7] Ding H., Liang J., The fundamental solutions for transversaly isotropic piezoelectricity and boundary element method, Computers & Structures, vol. 71, 1999, p. 447-455

[8] Dunn M.L., Micromechanics of coupled electroelastic composites: Effective thermal expansion and pyroelectric coefficients, Journal of Applied Physics, vol. 73, 1993, p. 5131-5140

[9] Enderlein M., Ricoeur A., Kuna M., Finite element techniques for dynamic crack analysis in piezoelectrics, International Journal of Fracture, vol. 134, 2005, p. 191-208

[10] Garcia-Sanchez F., Zhang Ch., Sladek J., Sladek V., 2-D transient dynamic crack analysis in piezoelectric solids by BEM, Computational Materials Science, vol. 39, 2007, p. 179-186

[11] Gruebner O., Kamlah M., Munz D., Finite element analysis of cracks in piezoelectric materials taking into account the permittivity of the crack medium, Eng. Fracture Mechahanics, vol. 70, 2003, p. 1399-1413

[12] Houbolt J.C., A recurrence matrix solution for the dynamic response of elastic aircraft, Journal of Aeronautical Sciences, vol. 17, 1950, p. 371-376

[13] Kuna M., Finite element analyses of cracks in piezoelectric structures – a survey, Archives of Applied Mechanics, vol. 76, 2006, p. 725-745

[14] Lee J.S., Boundary element method for electroelastic interaction in piezoceramics, Engineering Analysis with Boundary Elements, vol. 15, 1995, p. 321-328

[15] Lekhnitskii S.G., Theory of Elasticity of an Anisotropic Body, Holden Day, San Francisco, 1963

[16] Liu G.R., Dai K.Y., Lim K.M., Gu Y.T., A point interpolation mesh free method for static and frequency analysis of two-dimensional piezoelectric structures, Computational Mechanics, vol. 29, 2002, p. 510-519

[17] Mindlin R.D., On the equations of motion of piezoelectric crystals, problems of continuum, In: Mechanics 70th Birthday Volume (N.I. Muskelishvili, ed.), SIAM, Philadelpia, 1961, p. 282-290

[18] Mindlin R.D., Equations of high frequency vibrations of thermopiezoelasticity problems, International Journal of Solids and Structures, vol. 10, 1974, p. 625-637

[19] Nowacki W., Some general theorems of thermo-piezoelectricity, Journal of Thermal Stresses, vol. 1, 1978, p. 171-182

[20] Ohs R.R., Aluru N.R., Meshless analysis of piezoelectric devices, Computational Mechanics, vol. 27, 2001, p. 23-36

[21] Pak Y.E., Linear electro-elastic fracture mechanics of piezoelectric materials, International Journal of Fracture, vol. 54, 1992, p. 79-100.

[22] Qin Q.H., Fracture Mechanics of Piezoelectric

Materials, WIT Press, Southampton, 2001
[23] Qin Q.H., Mai Y.M., Crack growth prediction of an inclined crack in a half-plane thermopiezoelectric solid, Theoretical and Applied Fracture Mechanics, vol. 26, 1997, p. 185-191
[24] Rao S.S., Sunar M., Analysis of distributed thermopiezoelectric sensors and actuators in advanced intelligent structures, AIAA Journal, vol. 31, 1993, p. 1280-1286
[25] Saez A., Garcia-Sanchez F., Dominguez J., Hypersingular BEM for dynamic fracture in 2-D piezoelectric solids, Comput. Meth. Appl. Mech. Eng., vol. 196, 2006, p. 235-246
[26] Shang F., Kuna M., Kitamura T., Theoretical investigation of an elliptical crack in thermopiezoelectric material. Part I: Analytical development, Theoretical Applied Fracture Mechanics, vol. 40, 2003, p. 237-246
[27] Shang F., Kitamura T., Kuna M., Theoretical investigation of an elliptical crack in thermopiezoelectric material. Part II: Crack propagation, Theoretical Applied Fracture Mechanics, vol. 40, 2003, p. 247-253
[28] Sladek J., Sladek V., Atluri S.N., Meshless local Petrov-Galerkin method in anisotropic elasticity, CMES: Computer Modeling in Engn. & Sciences, vol. 6, 2004, p. 477-489
[29] Sladek J., Sladek V., Zhang Ch., Garcia-Sanchez F., Wunsche M., Meshless local Petrov-Galerkin method for plane piezoelectricity, CMC: Computers, Materials & Continua, vol. 4, 2006, p. 109-118
[30] Sladek J., Sladek V., Zhang Ch., Solek P., Starek L., Fracture analyses in continuously nonhomogeneous piezoelectric solids by the MLPG, CMES: Computer Modeling in Engn. & Sciences, vol. 19, 2007, p. 247-262
[31] Sosa H., Plane problems in piezoelectric media with defects, Int. J. Solids Structures, vol. 28, 1991, p. 491-505
[32] Tsamasphyros G., Song Z.F., Analysis of a crack in a finite thermopiezoelectric plate under heat flux, International Journal of Fracture, vol. 136, 2005, p. 143-166
[33] Tzou H.S., Ye R., Piezothermoelasticity and precision control of piezoelectric systems: Theory and finite element analysis, Journal of Vibration and Acoustics, vol. 116, 1994, p. 489-495
[34] Ueda S., Crack in functionally graded piezoelectric strip bonded to elastic surface layers under electromechanical loading, Theoretical Applied Fracture Mechanics, vol. 40, 2003, p. 225-236
[35] Zhu X., Wang Z., Meng A., A functionally gradient piezoelectric actuator prepared by metallurgical process in PMN-PZ-PT system, J. Mater. Sci. Lett., vol. 14, 1995, p. 516-518